Transition Metals Complexed to Ordered Mesophases.[1] Synthesis, Mesomorphism, and X-ray and EPR Characterization of a Homologous Series of *N*-(4-Dodecyloxysalicylidene)-4'-alkylanilines Complexed to Oxovanadium(IV)

Mauro Ghedini* and Stefania Morrone

Dipartimento di Chimica, Università della Calabria, I-87030 Arcavacata (Cs), Italy

Roberto Bartolino and Vincenzo Formoso

Dipartimento di Fisica, Università della Calabria, I-87030 Arcavacata (Cs), Italy

Oriano Francescangeli and Bin Yang

Dipartimento di Scienze dei Materiali e della Terra, Università di Ancona, I-60131 Ancona, Italy

Dante Gatteschi and Claudia Zanchini

Dipartimento di Chimica, Università di Firenze, I-50144 Firenze, Italy

Received June 2, 1992. Revised Manuscript Received February 24, 1993

A number of mesogenic bis[4-(dodecyloxy)-*N*-(4'-R_n-phenyl)salicylideneiminato]oxovanadium-(IV) complexes (**1-7**, R_n = CH_3, C_2H_5, C_3H_7, C_4H_9, C_6H_{13}, OC_6H_{13}, C_8H_{17}, respectively) have been synthesized and characterized by polarizing microscope observations, DSC measurements, X-ray diffraction, and EPR spectroscopy. These compounds are thermally stable and to not decompose on melting. Complexes **1-5** show two different solid phases K_1 and K_2. In addition, **4** and **5** exhibit a liquid-crystalline smectic A phase (monotropic in **4** and enantiotropic in **5**). On the other hand, **6** and **7** along with a single solid phase, display a smectic C (enantiotropic in **6** and monotropic in **7**) and an enantiotropic smectic A phase. Variable-temperature EPR spectra are accounted for on the basis of paramagnetic metal ions experiencing different magnetic environments. For each mesophase, matching X-ray, and EPR data, the molecular packing mode is suggested. Comparing **1-7** with the homologous copper complexes, the contribution of the metallic center to the mesomorphic properties is discussed.

Introduction

The study of new thermotropic liquid crystals containing transition-metal ions is an interesting topic because of the applicative and theoretical implications arising from the possible preparation of highly polarizable materials which display the specific properties associated with the different metals.[2] Mesogens with unusual features have recently been reported including the paramagnetic species obtained from copper(II)[3] or oxovanadium(IV).[4]

The role played by the metallic center M on the nature and the stability of the mesophase is not yet completely explored. However since a number of metallomesogens are bis-chelated complexes formed by salicylideneamine derivatives, RLH, insights about these points can be achieved from comparative investigations carried on homologous series of $(RL)_2M$ mesogens.

In a previous paper[3g] we reported on the synthesis, mesomorphic behavior, and EPR investigations of the copper(II) complexes obtained from the R_nLH Schiff bases of general formula shown in Chart I. For the sake of comparison, the same ligands have been employed for the preparation of the related $(R_nL)_2VO$ vanadyl derivatives.

The $(R_nL)_2Cu$ coordination compounds contain a tetracoordinated copper atom in a slightly distorted square planar geometry and display either monotropic or enantiotropic smectic phases characterized by a strongly interdigitated molecular array.[3g] In mesogenic species molecular geometry and mesomorphic character are as-

* To whom correspondence should be addressed.

(1) Part 11. Part 10: Ghedini, M.; Morrone, S.; Francescangeli, O.; Bartolino, R. *Chem. Mater.* **1992**, *4*, 1119.

(2) (a) Giroud-Godquin, A. M.; Maitlis, P. M. *Angew. Chem., Int. Ed. Engl.* **1991**, *30*, 375. (b) Espinet, P.; Esteruelas, M. A.; Oro, L. A.; Serrano, J. L.; Sola, E. *Coord. Chem. Rev.* **1992**, *117*, 215.

(3) Recent references: (a) Hoshino, N.; Murakami, H.; Matsunaga, Y.; Inabe, T.; Mariyama, Y. *Inorg. Chem.* **1990**, *29*, 1177. (b) Caruso, U.; Roviello, A.; Sirigu, A.; *Liq. Cryst.* **1990**, *7*, 421, 431. (c) Marcos, M.; Romero, P.; Serrano, J. L.; Barberà, J.; Levelut, A. M.; *Liq. Cryst.* **1990**, *7*, 251. (d) Marcos, M.; Romero, P.; Serrano, J. L.; *Chem. Mater.* **1990**, *2*, 495. (e) Bui, E.; Bayle, J. P.; Perez, F.; Liebert, L.; Courtieu, J. *Liq. Cryst.* **1990**, *8*, 513. (f) Pashche, R.; Balkow, D.; Baumeister, U.; Hartung, H.; Chipperfield, J. R.; Blake, A. B.; Nelson, P. G.; Gray, W. H. *Mol. Cryst. Liq. Cryst.* **1990**, *188*, 105. (g) Ghedini, M.; Morrone, S.; Gatteschi, D.; Zanchini, C. *Chem. Mater.* **1991**, *3*, 752. (h) Campillos, E.; Marcos, M.; Serrano, J. L.; Alonso, P. J. *J. Mater. Chem.* **1991**, *1*, 197. (i) Marcos, M.; Serrano, J. L. *Adv. Mater.* **1991**, *3*, 256. (j) Borchers, B.; Haase, W. *Mol. Cryst. Liq. Cryst.* **1991**, *209*, 319. (k) Sadashiva, B. K.; Ghode, A.; Rani Rao, P. *Mol. Cryst. Liq. Cryst.* **1991**, *200*, 187. (l) Thompson, N. J.; Gray, G. W.; Goodby, J. W.; Toyne, K. J. *Mol. Cryst. Liq. Cryst.* **1991**, *200*, 109. (m) Prasad, V.; Sadashiva, B. K. *Mol. Cryst. Liq. Cryst.* **1991**, *195*, 161. (n) Ohta, K.; Takenaka, O.; Hasebe, H.; Morizumi, Y.; Fujimoto, T.; Yamamoto, I. *Mol. Cryst. Liq. Cryst.* **1991**, *195*, 135. (o) Ohta, K.; Takenaka, O.; Hasebe, H.; Morizumi, Y.; Fujimoto, T.; Yamamoto, I. *Mol. Cryst. Liq. Cryst.* **1991**, *195*. 123.

0897-4756/93/2805-0876$04.00/0

Chart I

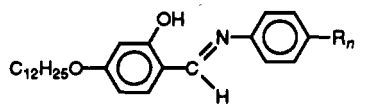

R_n = CH_3, C_2H_5, C_3H_7, C_4H_9, C_6H_{13}, OC_6H_{13}, C_8H_{17}

sociated so that for the $(R_nL)_2VO$ mesogens, in which the vanadium atom is pentacoordinated, mesomorphic properties somewhat different from those observed for the homologous copper compounds should be expected.

We wish to discuss here the contribution of the metal center to the mesomorphic behavior, referring to both its nature and coordination geometry.

Experimental Section

Synthesis of the Compounds. The syntheses of the R_nLH ligands were performed as previously described.[3g]

A typical procedure for preparation of the complexes 1–5 is given below.

Preparation of $(CH_3L)_2VO$, 1. To a suspension of CH_3LH (198 mg, 0.5 mmol) in ethanol (10 mL) were added potassium hydroxide (28 mg, 0.5 mmol) in ethanol (2 mL) and, dropwise, 2 mL of a warm ethanolic solution containing 63 mg (0.25 mmol) of vanadyl sulfate pentahydrate. The mixture was stirred at room temperature for 1 h; the resulting light green precipitate was filtered, washed with diethyl ether and recrystallized from chloroform–ethanol, yield 105 mg (50%). Anal. Calcd for $C_{52}H_{72}N_2O_5V$: C, 72.95; H, 8.48; N, 3.27. Found: C, 72.72; H, 8.68; N, 3.24. IR (KBr) ν (VO) 980 (s) cm^{-1}. All the analogous light green $(R_nL)_2VO$ complexes were prepared as described for 1. Yields, analytical data and V=O stretching frequencies are as follows:

$(C_2H_5L)_2VO$, 2: yield (56%). Anal. Calcd for $C_{54}H_{76}N_2O_5V$: C, 73.35; H, 8.95; N, 3.17. Found: C, 73.40; H, 8.90; N, 3.19 IR (KBr) ν (VO) 980 (s) cm^{-1}.

$(C_3H_7L)_2VO$, 3: yield (59%). Anal. Calcd for $C_{56}H_{80}N_2O_5V$: C, 73.73; H, 8.84; N, 3.07. Found: C, 73.53; H, 9.02; N, 3.03. IR (KBr) ν (VO) 980 (s) cm^{-1}.

$(C_4H_9L)_2VO$, 4: yield (63%). Anal. Calcd for $C_{58}H_{84}N_2O_5V$: C, 74.09; H, 9.00; N, 2.98. Found: C, 73.86; H, 9.34; N, 2.96. IR (KBr) ν (VO) 980(s) cm^{-1}.

$(C_6H_{13}L)_2$, 5: yield (56%). Anal. Calcd for $C_{62}H_{92}N_2O_5V$: C, 74.74; H, 9.31; N, 2.81. Found: C, 74.67; H, 9.70; N, 2.77. IR (KBr) ν (VO) 980(s) cm^{-1}.

Complexes 6 and 7 were prepared according to the following procedures.

$(C_6H_{13}OL)_2VO$, 6: To a solution of $C_6H_{13}OLH$ (100 mg, 0.207 mmol) in benzene (10 mL) was added 27 mg (0.103 mmol) of vanadyl acetylacetone. The mixture was stirred at room temperature for 12 h; the resulting green solution was concentrated, and the solid which precipitated was filtered, washed with diethyl ether, and recrystallized from chloroform–ethanol, yielding 50 mg (48%). Anal. Calcd for $C_{62}N_{92}N_2O_7V$: C, 72.41; H, 9.02; N, 2.72. Found: C, 71.94; H, 9.06; N, 2.59. IR (KBr) ν (VO) 980 (s) cm^{-1}.

$(C_8H_{17}L)_2VO$, 7: To a suspension of $C_8H_{17}LH$ (100 mg, 0.202 mmol) in ethanol (10 mL) was added 50 mg (0.101 mmol) of vanadyl acetylacetone. The mixture was stirred under reflux for 4 h; the resulting green solid was filtered, washed with diethyl ether, and recrystallized from chloroform–ethanol, yielding 55 mg (28%). Anal. Calcd for $C_{66}H_{100}N_2O_5V$: C, 75.29; H, 9.57; N, 2.66. Found: C, 74.64; H, 9.45; N, 2.64. IR (KBr) ν (VO) 980 (s) cm^{-1}.

Physical Measurements. The IR spectra (KBr pellets) were performed on a Perkin-Elmer 1330 spectrometer. Elemental analyses were obtained from the Microanalysis Laboratory of the Dipartimento di Chimica, Università della Calabria, Italy. The textures of the various mesophases were observed by means of a Ziess Axioscope polarizing microscope equipped for photography and with a Linkam CO 600 heating stage.

The calorimetric data were obtained by a DSC-2C Perkin-Elmer calorimeter and related data processor, at a heating rate of 5 °C min^{-1}. Aluminum containers of 20 μL capacity were used. Four calorimetric curves were recorded for each sample, heating and cooling down twice, in order to average out spurious effects.

The X-ray experiments were performed using a Rigaku Denki RV 300 rotating anode generator equipped with a conventional powder diffractometer and a small-angle high-resolution pinhole flat camera. Nickel-filtered Cu Kα radiation (λ = 1.54 Å) was used, strongly collimated with an appropriate slit system. The heating was achieved by a hot stage with accuracy ±0.5 °C and stability ±0.1 °C.

The EPR spectra were recorded at X-band frequency with a Bruker E-200 spectrometer in the temperature range −153 to 177 °C.

Results

Synthesis of the Complexes. The formation of bis-chelated complexes from salicylideneaniline derivatives and transition metal (II) ions is a straightforward process.[5] Accordingly also the reactions between the R_nLH ligands and vanadyl sulfate or acetylacetonate afford the complexes 1–7 as light green microcrystalline solids in good yields. These products were characterized by elemental analysis and IR spectroscopy where ν(V=O) at 980 cm^{-1} was detected for all compounds (Experimental Section).

In the solid state the pentacoordinated oxovanadium(IV) complexes can be found either as isolated molecules or as polymers containing hexacoordinated vanadium atoms as they form through V=O—V=O—interactions. Such an interaction gives rise to a lowering of the ν(V=O) stretching frequency[6,7] from 950–1000 to 800–850 cm^{-1}. The absence of such a shift in ν(V=O) for complexes 1–7 can be taken as an indication of a monomeric structure,[4i,8,9] however a hexacoordinated environment can be excluded also on the basis of the EPR data (vide infra).

As far as the coordination geometry is concerned, for pentacoordinated species two different arrangements, namely, trigonal bipyramidal and square pyramidal, should be considered. This bis(salicylideneiminato)oxovanadium(IV) complexes are usually assumed to be square pyramidal.[5] A similar geometry is suggested in the present case as well. The formula of complexes 1–7 is shown in Chart II.

Textural and Calorimetric Investigations. In 1–7 two anions arising from the mesogenic R_nLH molecules are coordinated to a vanadyl group. Their thermal behavior, determined by differential scanning calorimetry, is reported in Table I. Thus, compared to the R_nLH

(4) (a) Galyametdinov, Yu G.; Ivanova, I. V.; Ovchinnikov, I. V. *Zh. Obshch. Khim.* **1984**, *54*, 2796. (b) Galyametdinov, Yu. G.; Bikchantaev, I. G.; Ovchinnikov, I. V. *Zh. Obshch. Khim.* **1988**, *58*, 1326. (c) Serrano, J. L.; Romero, P.; Marcos, M.; Alonso, P. J. *J. Chem. Soc., Chem. Commun.* **1990**, 859. (d) Alonso, P. J.; Sanjuan, M. L.; Romero, P.; Marcos, M.; Serrano, J. L. *J. Phys.: Condens. Matter* **1990**, *2*, 9173. (e) Hoshino, N.,; Hayakawa, R.; Shibuya, T.; Matsumaga, Y. *Inorg. Chem.* **1990**, *29*, 5129. (f) Styring, P., Tantrawong, S.; Beattie, D. R.; Goodby, J. W. *Liq. Cryst.* **1991**, *10*, 581. (g) Hoshino, N.; Kodama, A.; Shibuya, T.; Matsumaga, Y.; Miyajima, S. *Inorg. Chem.* **1991**, *30*, 3091. (h) Barbera, J.; Levelut, A. M.; Marcos, M.; Romero, P.; Serrano, J. L. *Liq. Cryst.* **1991**, *10*, 119. (i) Serrette, A.; Carroll, P. J.; Swager, T. M. *J. Am. Chem. Soc.* **1992**, *114*, 1887.

(5) Vilas Boas, L.; Costa Pessoa, J. In *Comprehensive Coordination Chemistry*; Wilkinson, G., Gillard, R. D., Mc Cleverty, J. A., Eds.; Pergamon Press: Oxford, 1987; Vol. 3, pp 536–538.

(6) Mathew, M.; Carty, A. J.; Palenik, G. J. *J. Am. Chem. Soc.* **1970**, *92*, 3197.

(7) Farmer, R. L.; Urbach, F. L. *Inorg. Chem.* **1974**, *13*, 587.

(8) Pasquali, M.; Marchetti, F.; Floriani, C.; Merlino, S. *J. Chem. Soc., Dalton Trans.* **1977**, 139.

(9) Hamilton, D. E. *Inorg. Chem.* **1991**, *30*, 1670.

Table I. Thermal Behavior for the $(R_nL)_2VO$ Complexes 1–7

compd	transition temp (°C), enthalpies,[a] and mesophases[b]
1	$K_1 \xrightarrow{45.4^a} (100)K_2 \xrightarrow{13.1^a} (135)I \rightarrow K_2(120)$
2	$K_1 \xrightarrow{37.1^a} (85)K_2 \xrightarrow{24.7^a} (156)I \rightarrow K_2(144)$
3	$K_1 \xrightarrow{46.5^a} (94)K_2 \xrightarrow{16.2^a} (166)I \rightarrow K_2(158)$
4	$K_1 \xrightarrow{28.0^a} (80)K_2 \xrightarrow{32.8^a} (165)I \rightarrow S_A(156) \rightarrow K_2(132)$
5	$K_1 \xrightarrow{6.3^a} (85)K_2 \xrightarrow{18.7^a} (153)S_A \xrightarrow{9.3^a} (160)I \rightarrow S_A(159) \rightarrow K_2(130)$
6	$K \xrightarrow{31.12^a} (141)S_C \xrightarrow{0.23^a} (163)S_A \xrightarrow{11.11^a} (176)I \rightarrow S_A(175) \rightarrow S_C(162) \leftarrow K(110)$
7	$K \xrightarrow{29.43^a} (150)S_A \xrightarrow{12.31^a} (161)I \rightarrow S_A(158) \xrightarrow{0.12^a} S_C(142) \rightarrow K(130)$

[a] kJ/mol. [b] K = crystal, when two different solid phases are detected; K_1 indicates the solid phase stable over the lowest temperature range. S = smectic, I = isotropic liquid.

Chart II

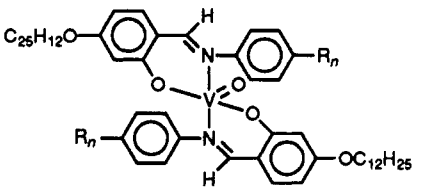

parents,[3g] the incorporation of a VO group between two R_nL moieties (Chart II) reduces the number of the mesophases and, as previously observed for the copper(II) compounds,[3g] increases the temperature at which the isotropic phase forms. Furthermore, the mesomorphic properties of the metal containing species are related to the length of the R_n alkyl chains. In particular, while for the shorter chains (i.e., compounds **1**, **2**, and **3** wherein R_n = CH_3, C_2H_5, and C_3H_7, respectively) only solid-to-solid transitions ($K_1 \rightarrow K_2$) are observed, for **4** ($R_n = C_4H_9$), **5** ($R_n = C_6H_{13}$), **6** ($R_n = OC_6H_{13}$), and **7** ($R_n = C_8H_{17}$) together with different solid phases, smectic phases (monotropic in **4** and enantiotropic in **5**–**7**) are detected. Complexes **1**–**7** are thermally stable and do not decompose upon melting.

Examinations of **4**–**7** by polarizing microscope showed in each case the typical fan-shaped texture[10] so that such smectic mesophases were classified as S_A. Moreover **6** and **7** display a further smectic phase (enantiotropic in **6** and monotropic in **7**) featured by the broken fan-shaped texture diagnostic of the S_C phase.[10]

The mesogenic vanadyl compounds are quite rare, and the only examples reported so far involve either substituted acetylacetone[4f] or salicylideneaminato ligands[4a–c,g,i]. In particular, those containing two salicylideneaminato derivatives as in **1**–**7** were complexes formed by *N*-(4-(heptyloxy)salicylidene)-4′-(octyloxy)aniline[4a,b] and the *N*-(4-(4-(decyloxy)benzoyloxy)salicylidene)-R (R = n-C_mH_{2m+1}: m = 1, 5, 10; R = $-C_6H_4OC_mH_{2m+1}$: m = 1, 2, 5, 10)[4c] or *N*-((4-R-benzoyloxy)salicylidene)-*n*-propylamine (R = $C_mH_{2m+1}O$: m = 5–12, 14, 16, 18)[4g] series. The corresponding mesogenic $(RL)_2VO$ complexes gave smectic A[4a,b] and smectic C[4c] or nematic phases;[4c,g] therefore, comparing these data with the behavior exhibited by **4**–**7**, it may be pointed out that the mesomorphism seems to depend mainly on the nature of the salicylidene-bonded substituents: S_A and S_C for alkoxy chains and N for the benzoyloxy groups.

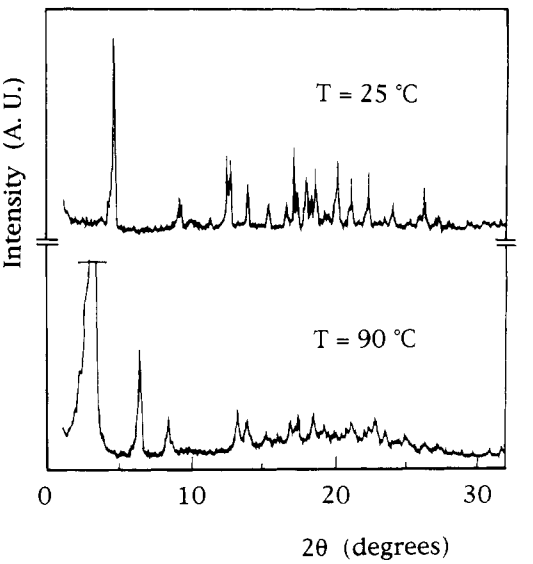

Figure 1. Compound **4**. X-ray diffraction patterns: K_1 (25 °C) and K_2 (90 °C) phases.

The calorimetric parameters of **1**–**7** are reported in Table I, these values being comparable with the literature data.[11]

X-ray Diffraction Study. The above-described mesomorphism was confirmed by X-ray measurements performed at different temperatures and under the first heating and cooling thermal cycle. However, as far as the solid phases are concerned, it should be noted that for samples which give $K_1 \rightarrow K_2$ transitions (i.e., **1**–**5**) K_1 is present only in the heating process of the virgin samples since in cooling from the isotropic melt the solid phase K_2 is stable down to room temperature, even for several days. Figures 1 and 2 report examples of the agreement between the diffraction patterns concerning the different phases and the phase diagrams reported in Table I.

(10) Demus, D.; Richter, L. *Texture of Liquid Crystals*; Verlag Chemie: Weinheim, Germany, 1978.

(11) Kelker, H.; Hatz, R. *Handbook of Liquid Crystals*; Verlag Chemie: Weinheim, Germany, 1980.

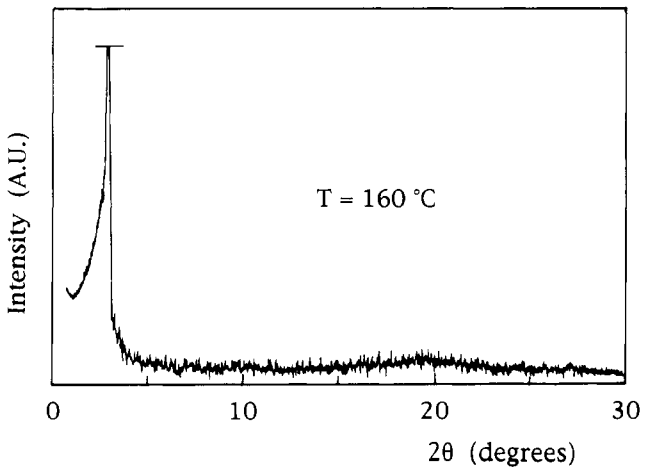

Figure 2. Compound 4. X-ray diffraction pattern: S_A (160 °C) phase.

In addition, with reference to the molecular array, the effects of the increasing of the temperature on the interlayer distance were considered.

Among the compounds which exhibit two solid phases, 5 behaves differently from the remaining complexes (1–4) as far as the interlayer periodicities, *d*, are concerned. In K_1 and *d* values are about 19 Å for 1–4 and 34 Å for 5, whereas in K_2, *d* results are in the 26–29-Å range for and 1–5 series. Therefore the compounds with the shortest R_n *n*-alkyl chains (1–4 for R_n = CH_3 to C_4H_9) in K_1 and in K_2 adopt two quite different molecular packings while 5 (R_n = C_6H_{13}) gives rise to similarly arranged K_1 and K_2 solid phases. The mesogens 6 and 7 show a unique K phase featured by $d \simeq 30$ Å. A similar periodicity is preserved in both the smectic C (6, 7) and A (4–7) mesophases; however, it is worthy of note that, paralleling the usually observed trend[12–15] the interlayer spacing, $d(S_C)$, slightly increases with the temperature.

EPR Spectra. EPR spectra of compounds 1–5 and 7 were recorded in the temperature range 25–180 °C.

For 1 the correspondence between X-ray and EPR data has been unambiguously checked by performing measurements on the same sample. The room-temperature spectrum of the freshly prepared compound is due to the K_1 phase and shows that an exchange narrowing process is operative (g = 1.998(3) and the peak-to-peak line width ΔB_{pp} = 200(10) G) with an incomplete averaging of the hyperfine structure. No evidence of a $K_1 \rightarrow K_2$ transition can be detected via EPR.

For 2–4 the room-temperature spectra of the freshly prepared compounds are typical of isolated VO^{2+}, with some interaction between the VO^{2+} species.

The spectrum of 2 is due to a quasi-axial vanadyl complex with g_{av} = 1.97, $A_{\parallel} \simeq 170$ G, and $A_{\perp} \simeq 60$–70 G, while the spectra of 3 and 4 show more anisotropic features with complicated structure due to incompletely resolved superhyperfine structure. The spectrum of 4 recorded at −63 °C is well resolved, showing, however, only a narrowing of the lines that makes easier the measurement of the splitting between them, but leaving the envelope unchanged. The room-temperature spectra recorded after the freezing treatment remains the same as those of freshly prepared samples, allowing us to conclude that no phase changes occur with decreasing temperature (down to −63 °C; see Figure 3a). The superhyperfine splitting, with $A \simeq 40$–50 G for both compounds, could be due to the interaction between neighboring vanadyl centers. This suggests the existence of an interaction between paramagnetic centers leading to clusters of vanadyl ions.

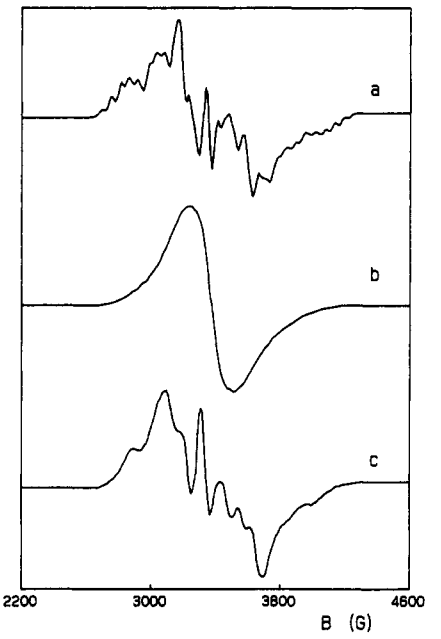

Figure 3. X-band EPR spectra of 4: a, K_1 solid phase (−63 °C); b, K_2 solid phase (100 °C); c, isotropic liquid phase (165 °C).

In agreement with the thermal behavior and the X-ray analysis these spectra can be attributed to the crystalline K_1 phase.

On increasing the temperature, the spectra of 2–4 narrow, and quasi-isotropic spectra are obtained at 85, 94, and 100 °C for 2 (g = 1.997(3), ΔB_{pp} = 165(10) G), 3 (g = 1.992(3), ΔB_{pp} = 210(10) G) and 4 (g = 1.990(5), ΔB_{pp} = 276(10) G), respectively. On the basis of the phase diagram these spectra can be attributed to the K_2 crystalline phase (see Figure 3b), allowing us to exclude that they can be determined by motional averaging. This suggests that an exchange narrowing process should be operative in the K_2 phases of 2–4, even if for 2 it appears to be not able to merge completely the hyperfine splitting.

For the compound 2 the room-temperature phase strongly depends on the preparation of the compounds and occasionally freshly prepared samples show the exchange narrowed spectra, which appear to be characteristic of the K_2 phases. In this case no evidence of a phase transition at the $K_1 \rightarrow K_2$ transition temperature is observed.

On increasing the temperature the isotropic liquid phase is obtained for all the 1–4 compounds and the EPR spectrum broadens showing a clear hyperfine structure (see Figure 3c). The spectrum is not isotropic, and this is due to the high viscosity of the liquid. The tumbling rate is probably sufficiently rapid to bring the lines to the position of the completely averaged spectrum (the hyperfine costant is ≃100 G), but the line width is different for each line, determining the appearance of the spectrum.

The smectic S_A phase of 4 is not clearly evidenced from its EPR spectrum, showing a spectrum similar, only with a broader line width, to that of the isotropic liquid.

(12) De Vries, *J. Phys.* **1975**, *36*, C-1, 1.
(13) De Vries, Abstract of the *Vth Int. Liquid Cryst. Conf. Stockolm*, 1974, 150.
(14) Doucet, J.; Levelut, A. M. *J. Phys.* **1977**, *38*, 1163.
(15) Doucet, J.; Levelut, A. M.; Lambert, M. *Mol. Cryst. Liq. Cryst.* **1973**, *24*, 317.

Table II. Summary of the Features Shown by the VO^{2+} Paramagnetic Center in 1–7 at Temperatures Corresponding to the Different Phases Detected by X-ray Measurements

		K	K_1	K_2	S_C	S_A	I	RT[a]
1	X-ray		d = 18.5 Å	d = 26.5 Å				K_2 (d = 27.0 Å)
	EPR		exchange narrowed	exchange narrowed			isotropic (highly viscous)[c]	
2	X-ray		d = 19.5 Å	d = 27 Å				K_2 (d = 27.5 Å)
	EPR		isolated moieties	exchange narrowed			isotropic (highly viscous)[c]	
3	X-ray		d = 18.2 Å	d = 27.2 Å				K_2 (d = 27.0 Å)
	EPR		isolated moieties	exchange narrowed			isotropic (highly viscous)[c]	
4	X-ray		d = 19.2 Å	d = 27.5 Å		d = 29.0 Å		K_2 (d = 31.0 Å)
	EPR		isolated moieties	exchange narrowed		quasi-isotropic[b]	isotropic (highly viscous)[c]	
5	X-ray		d = 34.5 Å	d = 29.0 Å		d = 31.0 Å		K_2 (d = 29.0 Å)
	EPR		exchange narrowed	exchange narrowed		quasi-isotropic[b]	isotropic (highly viscous)[c]	
6	X-ray	d = 30 Å			d = 29.7[d]	d = 30.7		K (d = 30.0 Å)
	EPR	exchange narrowed			quasi-isotropic[b]	quasi-isotropic[b]	isotropic (highly viscous)[c]	
7	X-ray	d = 30 Å			d = 30.3[e]	d = 31.2		K (d = 30.0 Å)
	EPR	exchange narrowed			quasi-isotropic[b]	quasi-isotropic[b]	isotropic (highly viscous)[c]	

[a] Room temperature after the thermal treatment. [b] Not clearly distinguishable from that of the isotropic liquid. [c] See Figure 3c. [d] Value at 150 °C. [e] Value at 140 °C.

On cooling, the spectra narrow, and at room temperature after the thermal treatment, all the 1–4 compounds show the spectra of the K_2 solid, unchanged after 1 day.

The room-temperature X-band EPR spectrum (25 °C) of 5 consists of a broad, asymmetric and featureless signal centered at g = 1.993(3) with ΔB_{pp} = 290(10) G. In the K_1 phase an exchange pathway should be operative, but it appears less effective than that observed in other complexes of the series. The spectrum of the K_2 phase is observed at 85 °C and shows an asymmetric feature with an incompletely resolved hyperfine structure. This structure is lost on increasing the temperature up to 150 °C, where a broad featureless signal centered at g = 1.995(3) with ΔB_{pp} = 290(10) G is observed. At 153 °C, where the $K_2 \rightarrow S_A$ transition is observed, the EPR spectrum shows a resolved hyperfine structure. The spectrum of the isotropic liquid is observed at 160 °C. The phase diagram indicates the reversibility of the transition between the smectic phase and the isotropic liquid and this behavior is confirmed by the EPR measurement. The spectrum observed at 153 °C on increasing temperatures seems to correspond, however, to a superposition of two spectra, those of the smectic phase and the isotropic liquid. During the thermal treatment, the smectic phase is present in a small range of temperature (153–160 °C) and the inhomogeneity of the warming could determine this effect. On decreasing the temperature, the S_A phase is present for a larger temperature range (160–130 °C), and the spectrum attributable to it is stable from 157 to 137 °C. On cooling, the spectrum loses the resolved hyperfine structure, and at room temperature, after the thermal treatment, the spectrum of the K_2 phase is observed.

Complexes 6 and 7 display similar phase diagrams. The temperature dependence of the ESR spectra of compound 7 confirms the results of the optical microscopy. The room-temperature spectrum of the freshly prepared compound is typically exchange narrowed (with g = 1.989(3) and ΔB_{pp} = 197(2) G). At 151 °C a spectrum that strongly resembles that observed for the S_A phase of compounds 4 and 5 arises, evolving at 160 °C to that of the isotropic phase. On cooling, a clear change occurs at 151 °C, and the observed spectrum remains unchanged down to 130 °C, where an exchanged spectrum reveals the presence of a crystalline phase.

No attempt was made to fit the experimental spectra. A large number of highly correlated parameters should be used in the calculations, namely, the three g values, the three hyperfine constants, and the three related anisotropic line widths, and, having no possibilities to independently check them, reasonable agreement with the experiment can be found with different sets of values, all exhibiting a very small in plane anisotropy of the g, A, and line-width values.

Discussion

The actual environments experienced by the VO^{2+} paramagnetic centers and the layer periodicities should be diagnostic of the molecular packing, and a comparison between EPR and X-ray measurements is summarized in Table II.

EPR data concerning VO^{2+} compounds mainly deal with measurements carried on solutions, while fewer data are reported for samples in the solid state.[16,17] In addition, the VO^{2+}-containing liquid crystalline species investigated so far display mesophases different from those detected for 1–7; therefore, the only comparisons allowed by the literature data refer to bis[4-((4-(decyloxy)benzoyl)oxy)-*N*-(4′-(*n*-pentyloxy)phenyl)salicylideneiminato]oxovanadium(IV), I, either as solid or isotropic liquid,[4d] and to bis[4-((4-(decyloxy)benzoyl)oxy)-*N*-(4′-*n*-pentyl)-salicylideneiminato]oxovanadium(IV), II, as solid.[4d] Worthy of note, both I and II give room-temperature spectra which look like those recorded for 2–4 in the K_1 phase, and I, as an isotropic liquid, shows spectral features as found for 1–7. On the contrary, on cooling the isotropic liquids to room-temperature I restores the spectrum of the pristine solid, while 1–7 show the spectra characteristic of the K_2 or K phases.

The mesogenic series which comprises I and II has been studied using X-ray diffraction methods,[4h] and the obtained findings for the nematic phase agree with a molecular arrangement in which neighboring molecules are partially interdigitated without any evidence of local coupling of molecules in pairs or in ribbons in a side by side array. Actually no evidences of magnetic exchange were supplied by the EPR analysis.[4d]

The complexes 1–7 give the X-ray and EPR results shown in Table II; therefore, in order to account for the

(16) Syamal, A. *Coord. Chem. Rev.* **1975**, *16*, 309.
(17) Bencini, A.; Gatteschi, D. *Transition Met. Chem. (N.Y.)* **1982**, *8*, 1.

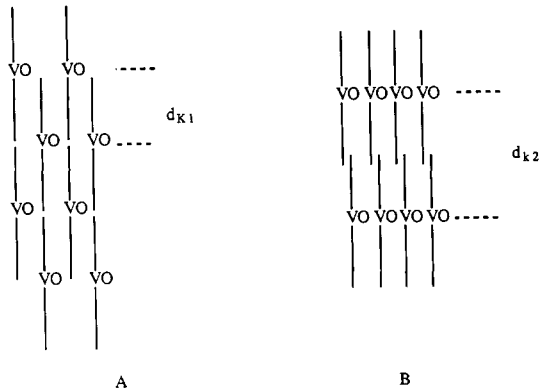

Figure 4. Complexes 1–4: sketch of the molecular array in the K_1 (A) and K_2 (B) solid phases.

observed magnetic exchange and layer periodicities, 1–4 can be collected in a single group since 5–7 (the complex bearing the longest R_n alkyl chain) show peculiar features as far as the K_1 (5) or K (6,7) phase is concerned.

The never thermally treated polycrystalline samples, 2–4, except for 1, exhibit room-temperature EPR spectra indicating isolated VO^{2+} centers and interlayer periodicities [$d(K_1)$ = 19 Å] much smaller than the theoretical molecular lengths (about 42 Å). Upon heating, reaching the K_2 phase, the layer thickness , $d(K_2)$, increases to 26–29 Å and a magnetic exchange becomes apparent. Approaching the isotropic liquid phase (and throughout the smectic A phase for compound 4) the exchange process becomes less effective and in some extent it is also operative in the melted samples. Cooling to room temperature, the isotropic liquid freezes in the K_2 phase.

Tentatively, a way to reconcile the EPR and X-ray data is to suppose that in K_1 the molecular layers consist of strongly interdigitated molecules (Figure 4A) magnetically interacting (1) or noninteracting (2–4), and when the K_2 transition takes place, the molecules rise perpendicularly to the layers, $d(K_2) > d(K_1)$ (Figure 4B) allowing the magnetic exchange interaction probably through the alkyl chains.[18] On increasing the temperature further the magnetic exchange is progressively lost, probably because of the increased molecular motions. When the melting point is reached, the hyperfine structure due to an isotropic high-viscosity liquid appears. The molecular arrangement exhibited by the fluid phase is approximately preserved in K_2; consequently, cooling from the isotropic liquid phase to room temperature, the K_2 solid phase forms. On the contrary, K_1 is not restored. In light of this model, the results obtained for 5–7 can be similarly described since the only difference between 1–4 and 5 is in the K_1 phase [i.e., $d(K_1) > d(K_2)$] and both the EPR spectrum and the $d(K_1)$ or $d(K)$ values account for a structure like that depicted in Figure 4B.

The thermodynamic parameters concerning the $K_1 \rightarrow K_2$ transitions (Table I) seem to support the proposed molecular packings. Indeed while the calculated ΔH for 1–4 compounds are the 28.0–46.5 kJ mol^{-1} range, the large difference between 1–4 and 5 ($K_1 \rightarrow K_2$: ΔH = 6.3 kJ mol^{-1}) provides evidence for a dramatic structural modification which in 1–4 is associated with the $K_1 \rightarrow K_2$ transition.

The $(R_nL)_2VO$ species 1–7 are formed by R_nL moieties as in the previously reported $(R_nL)_2Cu$ complexes.[3g] In these compounds both the VO(II) and Cu(II) ions impose a roughly square-planar coordination geometry; however, since the oxygen atom of the vanadyl group occupies an apical position, the coordination geometries that actually result are distorted square pyramidal for $(R_nL)_2VO$ and distorted square planar for $(R_nL)_2Cu$. Thus, in matching the mesomorphic properties of a homologous series of $(R_nL)_2VO$ and $(R_nL)_2Cu$ complexes, the influence of the metallic center (i.e., VO(II) and Cu(II)) can be stressed. For the sake of comparison the data concerning the appropriate copper complexes together with those for vanadyl have been plotted in Figure 5.

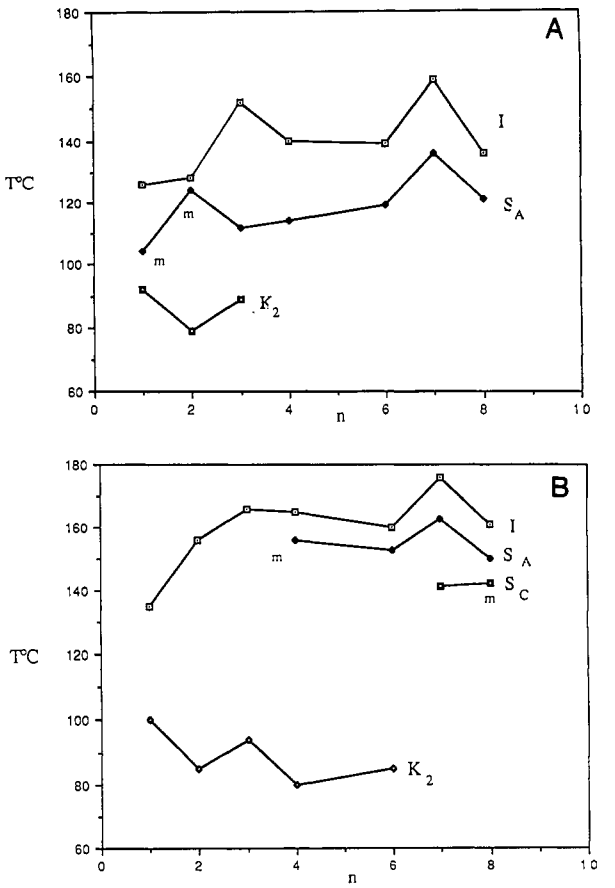

Figure 5. Plots of mesomorphic transition temperatures versus the R_n alkyl chain length (n) for copper (A) (from ref 3) and vanadyl (B) complexes. I = isotropic phase; S = smectic phase; K = solid phase; m = monotropic transition.

With reference to the mesophases, both series display similar features (e.g., only $K_1 \rightarrow K_2$ or $K_2 \rightarrow S$ transitions), although the temperatures at which the transitions occur are generally higher for $(R_nL)_2VO$ than for $(R_nL)_2Cu$ (Figure 5).

The molecular packing of the copper mesogens has been extensively investigated[3g,19] and a strongly interdigitated structure has been proposed. Since for 1–7 in any mesophase the calculated periodicities (d) are shorter than the theoretical molecular lengths (vide supra), probably these compounds also adopt a similar structure (Figure

(18) Bencini, A.; Gatteschi, D. *EPR of Exchange Coupled Systems*; Springer Verlag: Berlin, 1990.

(19) (a) Ghedini, M.; Armentano, S.; Bartolino, R.; Torquati, G.; Rustichelli, F. *Solid State Commun.* **1987**, *64*, 1191. (b) Levelut, A. M.; Ghedini, M.; Bartolino, R.; Nicoletta, F. P.; Rustichelli, F. *J. Phys.* **1989**, *50*, 113. (c) Albertini, G.; Guido, A.; Mancini, G.; Stizza, S.; Ghedini, M.; Bartolino, R.; *Europhys. Lett.* **1990**, *12*, 629. (d) Bartolino, R.; Rustichelli, F.; Scaramuzza, N.; Versace, C. C.; Ghedini, M.; Pagnotta, M. C.; Armentano, S.; Ricci, M. A.; Benassi, P. *Solid State Commun.* **1991**, *80*, 587.

4); therefore, the higher temperatures at which the transitions occur and the longer R_n alkyl tails necessary to bring about the S_C or S_A phases could be ascribed to stronger intermolecular interactions exerted by the rigid molecular core formed by the VO(II) coordination sphere and the four aromatic rings (Chart II).

Other comparative studies carried out on vanadyl and copper mesogens have been recently reported by Hoshino et al.[4e,g] and by Serrano et al.[4h] Both groups reported on substituted salicylideneiminato complexes, of general formula $(RL)_2M$ (M = Cu, VO), which display nematic mesophases. Nevertheless, the resulting trend both for the temperatures at which the mesophases appear and for the melting points is Cu(II) > VO(II) for bis[4-((4-alkoxybenzoyl)oxy)-*N*-(*n*-alkyl)salicylideneiminato] complexes[4e,h,g] and VO(II) > Cu(II) for the bis[4-((4-(decyloxy)-benzoyl)oxy)-*N*-(4′-methoxyphenyl)salicylideneiminato] complex (III).[4h] Hoshino explained the Cu(II) > VO(II) result suggesting that the oxygen of the VO group, which should occupy the apical position of a square-pyramidal coordination geometry, would increase intermolecular separation in the nematic phase. Consequently the transition temperatures[4f] of the vanadyl complexes are lower than those of the homologous copper mesogens. The results described in this work deal with bis[4-(dodecyloxy)-*N*-(4′-alkylphenyl)salicylideneiminato] complexes and give VO(II) > Cu(II) (Figure 5). Thus, comparing III with 1–7 it seems possible to recognize that VO(II) > Cu(II) when the N-bonded fragment bears a phenyl ring. Albeit such a statement requires further examples in order to be considered as a general rule, the mesomorphic behavior displayed by 1–7 confirms that the VO group is carrier of strong intermolecular interactions which need to be properly balanced by flexible substituents so that mesomorphic properties are present in bis-(salicylideneiminato)oxovanadium(IV) complexes.

Acknowledgment. This work was supported by the Italian Consiglio Nazionale delle Ricerche (CNR) under the cover of "Progetto Finalizzato Materiali Speciali per Tecnologie Avanzate".